Root Locus Based Autopilot PID's Parameters Tuning for a Flying Wing Unmanned Aerial Vehicle

Fendy Santoso, Ming Liu & Gregory Egan

Department of Electrical & Computer Systems Engineering
Monash University, VIC, 3800
Melbourne, Australia
fendy.santoso@gmail.com, ming.liu@eng.monash.edu.au

Abstract. This paper depicts the applications of classical root locus based PID control to the longitudinal flight dynamics of a Flying Wing Unmanned Aerial Vehicle, P15035, developed by Monash Aerobotics Research Group in the Department of Electrical and Computer Systems Engineering, Monash University, VIC, Australia. The challenge associated with our UAV is related to the fact that all of its motions and attitude variables are controlled by two independently actuated ailerons, namely elevons, as its primary control surfaces along with throttle, in contrast to most conventional aircraft which have rudder, aileron and elevator. The reason to choose PID control is mainly due to its simplicity and availability. Since our current autopilot, MP2028, only provides PID control law for its flight control, our design result can be implemented straight away for PID parameters' tuning and practical flight controls. Simulations indicate that a well-tuned PID autopilot has successfully demonstrated acceptable closed loop performances for both pitch and altitude loops. In general, full PID control configuration is the recommended control mode to overcome the adverse impact of disturbances. Moreover, by utilising this control scheme, overshoots have been successfully suppressed into a certain reasonable level. Furthermore, it has been proven that exact pole-zero cancellations due to derivative controls in both pitch and altitude loop to eliminate the effects of integral action -contributed by open loop transfer functions of elevon-average-to-pitch as well as pitch-to-pitch-rate- is impractical.

1   Introduction

The ultimate design that the UAV engineers wish to achieve is to provide autonomous systems from taking off, cruising to landing. The development of small UAVs have been expanded rapidly for various purposes starting from hobbyist such as radio controlled aircraft, up to military applications, e.g., spy aircraft. Such aircraft have been developed rapidly, mainly after World War I, and applied by some countries during World War II. The interest of such

aircraft has grown significantly due to the advantages they offered, e.g., more economical to operate and no risk of aircrews [1-4].

It has been established beyond doubt that in recent years we have witnessed a massive researches and developments for uninhabited air vehicles. Recent research regarding to GPS-based autopilot for a UAV can be found in [5]. Meanwhile, the implementation of multivariable autopilot for a small helicopter can be found in [6]. Also, the development of novel autopilot for a UAV with auto-lockup capability has been discussed in [7]. Furthermore, prior research due to the implementation of robust H_2 and H_∞ as well as gain scheduled autopilots have been rigorously discussed in [1], [8-10].

This paper nonetheless rigorously discusses the study of applying root locus based PID autopilot to the altitude control for a particular aircraft that has elevon control surfaces only. Our early identification work for the aircraft has been published in [4] with extensions to this work in [1-3].

The UAVs of our interest are small and fly at relatively low Reynolds Numbers (250K) regimes which, amongst other challenges, mean turbulent flow and laminar separation across wing surfaces. Partially due to this reason, the aircraft dynamics are non-linear and at times uncertain. Aircraft of this size are also very susceptible to air turbulence [1-3].

Based on the open loop model elevon-average-to-altitude acquired, PID autopilots have been subsequently designed. The first reason to choose PID is due to its simplicity. Since it does not require such complicated computations, it can be implemented by a cheap and affordable payload for a small aircraft. This, of course, leads to smaller demands of memory and processor capacity. The second reason is due to its availability. Since our UAV, P15035, from Monash Aerobotics Research Group has already employed onboard PID controllers for its autopilot; our design results can be implemented straight away.

Relevant control theory could be found in [11-28] with special emphasis on system identification techniques can be found in [21-27]. We have at our disposal a very large repository of flight logs for our aircraft obtained over several years. The logs contain a complete record of aircraft in-flight dynamics. It is intended to make this material available to other researchers for their control system studies.

The availability of control systems toolbox in MatLab makes the composition process become a rather easy task; the offline algorithms are significantly more

computationally intensive than the simple PID based control loops computed online or in-flight, where we have electrical and computational power limitations.

The organisation of this paper is as follows. The derivation of the open loop longitudinal model is given in Section II. Furthermore, the performances of single control modes, i.e., single P, I and D autopilot are given in Section III. Subsequently, the possible combination of 2 control modes will be studied, i.e., Proportional Integral modes as well as proportional differential modes. Finally the performances of full PID control configurations will also be examined. Discussions and conclusions are then made accordingly in Section IV.

2   The Open Loop Longitudinal Model

Generating a comprehensive non-linear mathematical model for an aircraft is usually impractical. Instead, a more realistic approach is to develop a linearised model which is valid for a small dynamic range. Longitudinal and lateral models for conventional larger aircraft are well understood [29-34].

Most conventional aircraft have three primary control surfaces, namely, rudder, elevator and ailerons. Along with the throttle they are the four major input variables to control the flight of an aircraft. The aircraft used in this study (Figure 1 and Table 1) is a flying wing and if unswept it is known as a "plank" because of its resemblance of course to a plank of wood. Most flying wings have only two control surfaces or elevons that combine the function of ailerons for roll control (and indirectly turn) and elevators for pitch control [1-3].

Planks are simple to construct and can be made to be very compact, rugged and crash tolerant. The flight characteristics of planks are benign, at least for human operators and they also exhibit predictable stall behaviour allowing them to descend quickly and safely. All of these characteristics were important in the design of P15035, its sister aircraft P16025 and the superficially similar Dragon Eye now widely deployed with the US Marines [1-3].

Flying wings, because they do not have a tail, rely on some reverse camber (upsweep in the trailing edge of the wing) to maintain a zero pitching moment and with that comes drag and less energy efficiency. To minimise the reverse camber we have to minimise the stability margin in the pitch axis. In this study, the stability margin has been made sufficiently high to allow human control. The controller described here will permit us to use airfoils with less camber and less drag both for computer assisted and autonomous flight [1-3].

Figure 1 The P15035 Aircraft (Reproduced with the permission of J. Bird a member of the Aerobotics Group).

Pitch is controlled by the average deflection of the two elevons and rolls (and indirectly yaw) by the difference, at least to a first order approximation. It is worth noting that for planks roll is normally controlled by deflecting the elevons equally in an attempt to control yaw and to again minimise unnecessary drag. It is feasible to control the elevons independently in a more optimum fashion rather than have them coupled in a relatively simple relationship. This will be developed further in later research, but for now, we will concentrate on pitch-axis control where the elevons are driven in unison.

Table 1   Specifications of Aircraft P15035.

Span	150 cm	Motor	Electric
Chord	35 cm	Duration	40-60 minutes
Length	106 cm	Speed	33 to 150 Kph
Control Surface	Elevon	Battery	28×GP3300 NiMh
Weight	2.9 to 4.6 kg	Autopilot	MP2028

The longitudinal model and lateral directional model for the P15035 have been obtained using system identification techniques [19-21] based on real flights, as distinct from simulation, and were initially reported in [4].

For trimmed flight with a constant engine thrust (and airspeed) the P15035's longitudinal discrete time transfer function from the elevon average deflection ∂ (degree) to the pitch angle $\theta\,(°)$ with a sampling frequency of 5 Hz is

$$\frac{\theta}{\delta} = \frac{-0.13065\,z^2\,(z+0.0091)}{(z-0.9115)(z-0.9785)(z^2+0.2267\,z+0.3763)}. \tag{1}$$

Converted to s domain, it becomes:

$$\frac{\theta(s)}{\delta(s)} = \frac{-0.2954(s+6.693)(s^2+11.7s+91.49)}{(s+0.4633)(s+0.1087)(s^2+4.887s+83.12)}. \qquad (2)$$

In which, its complex conjugate poles are: $s=-2.4435 \pm 8.7835i$. It is apparent that as all poles of (2) are located on the left hand side of the s plane so the open loop system is stable as we expect.

It has been established (e.g., see [5], [11-12], [27-30]) that the typical longitudinal dynamics of a traditional aircraft (elevator to pitch) with a constant engine thrust can be expressed as

$$\frac{\theta(s)}{\delta(s)} = \frac{k_\theta \left(s+1/T_{\theta_1}\right)\left(s+1/T_{\theta_2}\right)}{(s^2+2\varsigma_p\omega_p s+\omega_p^2)(s^2+2\varsigma_s\omega_s s+\omega_s^2)}, \qquad (3)$$

where δ is now the elevator angle (instead of the elevon average in (2)). For aircraft, the factor $\Delta s_p = s^2 + 2\varsigma_p\omega_p s + \omega_p^2$ in the characteristic equation of (3) is termed the phugoid mode and the second one $\Delta s_s = s^2 + 2\varsigma_s\omega_s s + \omega_s^2$ is the short period mode. Typically, the phugoid mode is lightly damped with a relatively large period and the short period mode represents heavily damped oscillation. As a result, phugoid roots are always complex conjugate located near the origin. In our case, nevertheless, the overall pitch step response is a combination of a slow exponential function and a quickly decaying high frequency oscillation

Comparing (2) with (3), it can be apparently seen that the longitudinal model (2) has pitch characteristics which are not similar to those of conventional aircraft. Consequently, when the roots are real, the term phugoid can no longer be properly used. In our case, its phugoid model is replaced by pitch subsidence roots and is given by:

$$\Delta s_p = (s+0.4633)(s+0.1087). \qquad (4)$$

This is overdamped with a dominant large time constant of $\tau = 10s$. Its short period model is given by:

$$\Delta s_s = s^2 + 4.887s + 83.12. \qquad (5)$$

Here, the damping ratio is about 0.268 and the natural frequency 9.12 rad/s. The settling time is small being in the order of 1s. The impulse response for both modes is plotted in Figure 2. Normally, the roots of the phugoid mode are complex conjugate. In this research we have nonetheless encountered a different situation.
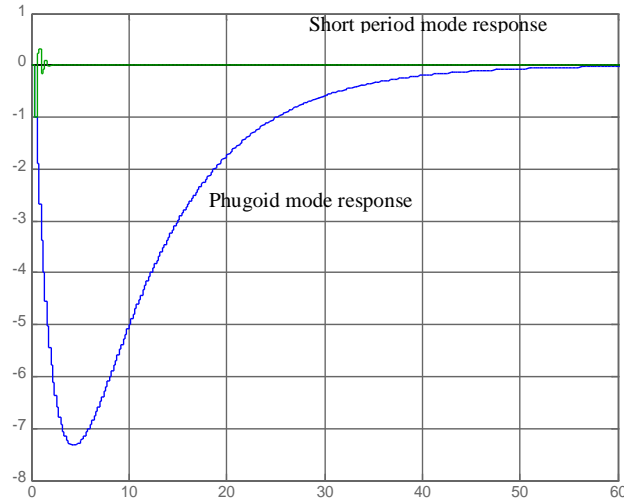
Figure 2 Impulse pitch amplitude response in degrees for phugoid and short period modes of UAV P15035.

Having confirmed the fact that the longitudinal response is of the general form expected, we now determine the pitch-to-altitude transfer function in *z* domain with a sampling frequency of 5 Hz as:

$$\frac{h(z)}{\theta(z)} = \frac{0.05456\,z}{z - 0.9969}\,. \tag{6}$$

Eventually, converting (6) to *s* domain and cascading it with (2), we obtain the following transfer function:

$$\frac{h}{\delta} = \frac{-0.011659\,(s^2 + 11.88s + 42.46)(s^2 + 9.723s + 99.83)}{(s + 0.4633)(s + 0.1087)(s + 0.01552)(s^2 + 4.887s + 83.12)}\,, \tag{7}$$

where, *h* is the altitude of the aircraft in metres.

3   PID Autopilot Designs

The "double loop" autopilot structure is clearly depicted in Figure 3.
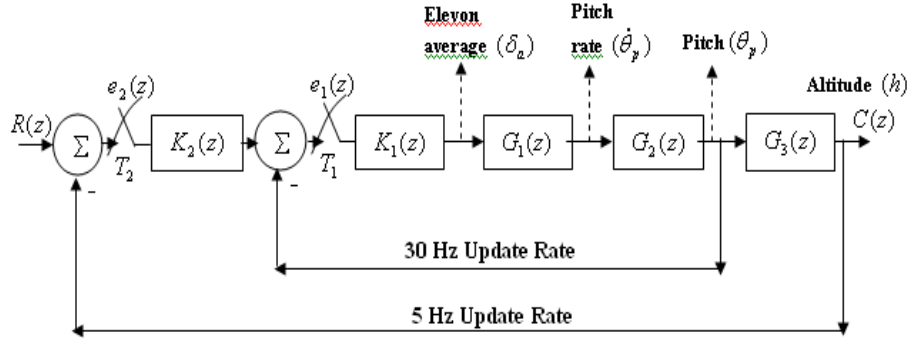
Figure 3 Control Loop of Longitudinal Motion.

A well-known method employed by control engineers in practise is the so-called "Ziegler-Nichols" tuning. It works based on quarter decay ratio responses. Nevertheless, since the design objective of this research is to minimise overshoots whilst still maintain a reasonably fast settling time, this tuning method could not become a suitable candidate for controlling an aircraft.

An aircraft, in fact, is quite sensitive to overshoots, particularly when it wants to descend or land. A reasonable amount of overshoots could create severe damages to the systems and indeed suppress the efficiency of the closed loop control systems. As a result, we have conceived choosing root locus technique in allocating the closed loop poles since it can accommodate a lot more degree and flexibility in adjusting the closed loop poles. Other viable techniques for tuning the PIDs gain in the literature exist, including the use of fuzzy systems, neural networks or coefficient diagram method [6].

3.1   Proportional Autopilot

The transfer function of a proportional control in z domain is based on a single amplification (constant gain) as follows:

$$U(z) = K_p e(z) . \tag{8}$$

The gain of a proportional control can be treated as the gain of root locus. It turns out that:

$$K_p = K_{rl} ,$$

where, K_{rl} is the gain of root locus.

Since proportional control cannot create any significant changes on the root locus topology what can be achieved instead to improve the desired closed loop

performances is only to adjust the proportional gain to yield to the acceptable closed loop performances. The main advantage of this control scheme is in fact due to its simplicity.

The fact that the open loop transfer function of elevon-average-to-pitch in practice is not a perfect type one system shall lead this control scheme to poor disturbance rejection and also the inevitable amount of steady state error, especially for small value of proportional gains.

The pitch responses for numerous value of K_p (small gain between 1 to 10) are given by Figure 4.
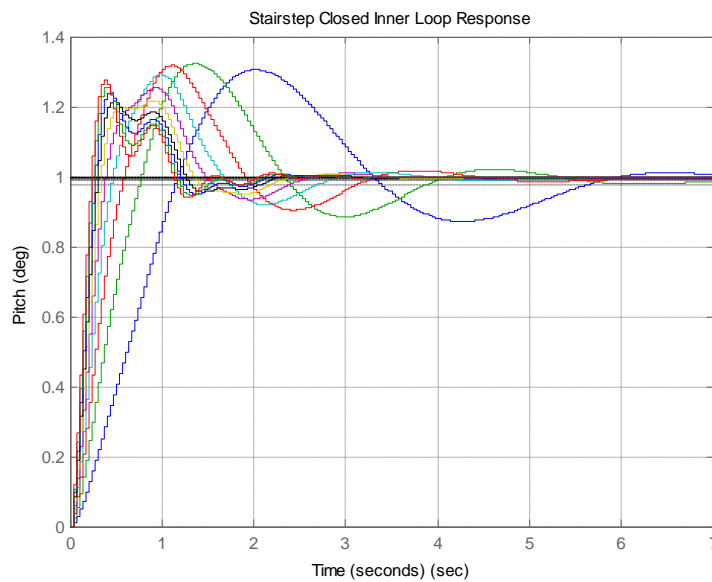
Figure 4 Pitch Response Due to Unit Step Input.

Accordingly, the resulting altitude responses with respect to a constant set point for various K_p are given by Figure 5.
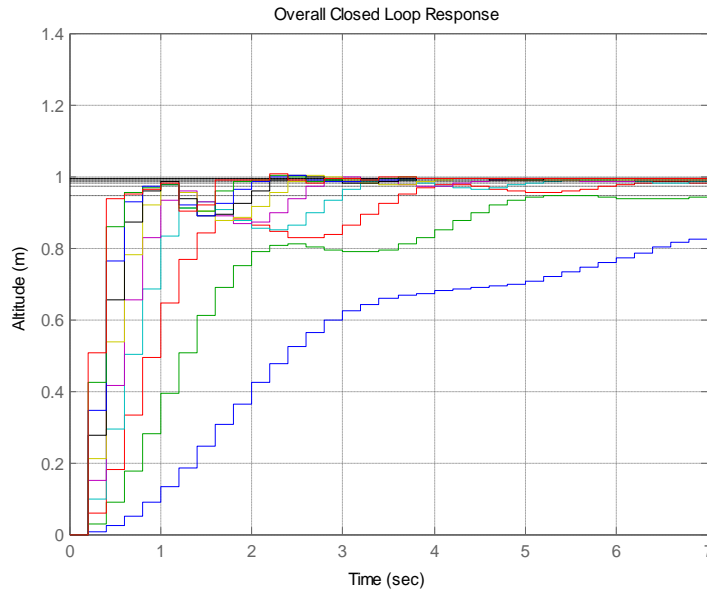
Figure 5 Altitude Loop Response.

It is obvious that according to (7) the open loop transfer function of elevon-average-to-altitude is neither a perfect type one nor a type two system. Accordingly, the steady state error has been an inevitable outcome.

The value of steady state error can be calculated using the following equation

$$e_{ss} = \frac{1}{1+K_p}. \tag{9}$$

In which K_p known as position constant and is defined as:

$$K_p = \underset{s \to 0}{Lim}\{K(s)G(s)\}. \tag{10}$$

It is now apparent from (9) and (10) that the higher the value of proportional gains, the smaller the value of steady state error and vice versa. Proportional gain in fact must be carefully chosen as a delicate balance of trade off between steady state error and overshoots as illustrated in Figure 6.
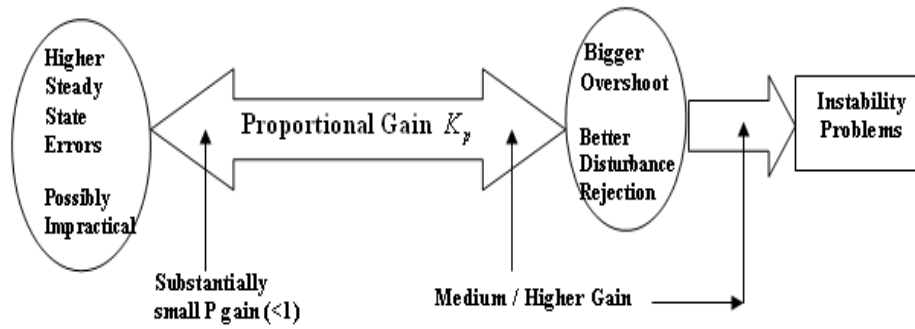
Figure 6 Constrains in Choosing an Appropriate Proportional Gain K_p.

3.2 Integral Autopilot

The time domain performances of integral controls are investigated in this section. The transfer function of an integrator in z domain can be depicted as follows:

$$K(z) = K_i \frac{Tz}{(z-1)}, \tag{11}$$
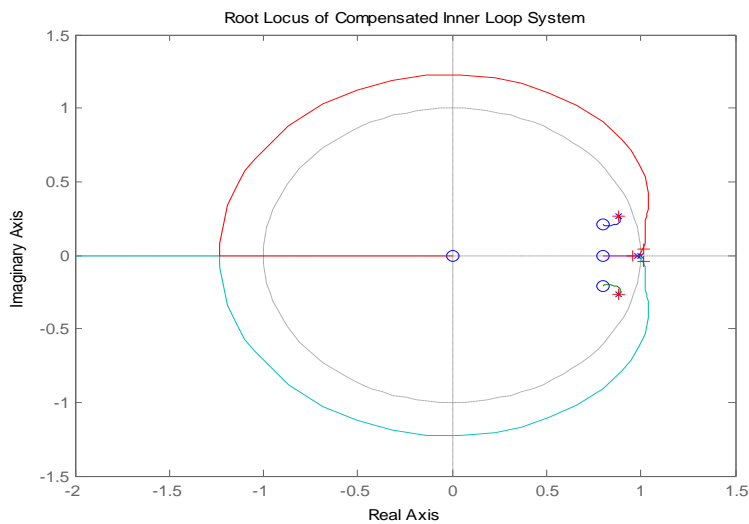
where, K_i : Integral gain,

T : Sampling period.

Figure 7 Unstable Pitch Root Locus.

Consequently, irrespective of the value of chosen integral gain K_i, it shall contribute one zero at $z = 0$ as well as one pole at $z = 1$. Unfortunately, the open loop transfer function of elevon-average-to-altitude has already had two poles around $z = 1$. Thus, the additional pole from integral control will tend to push the branches of the the root locus out of the unit circle. As a result, it shall create instability problems as given by Figure7 and Figure 8 respectively.
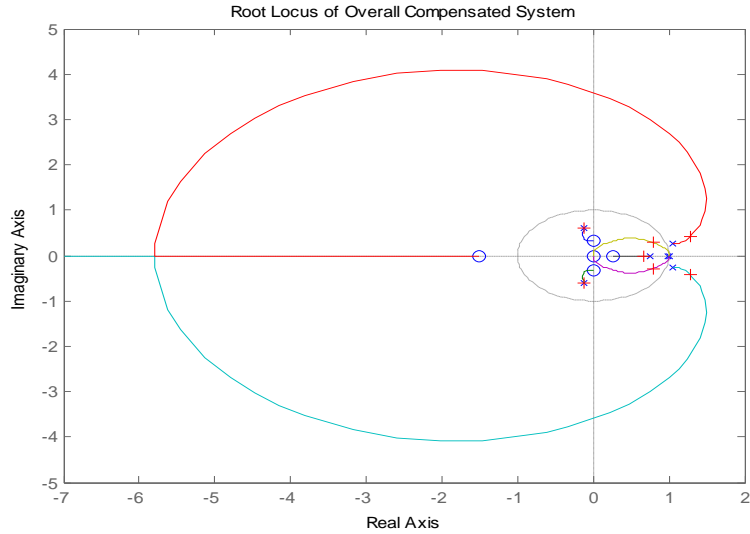

Figure 8   Unstable Altitude Root Locus.

3.3   Exact Pole/Zero Cancellation Issues due to DD Control

We could argue that theoretically we may be able to cancel the double poles located at $z = 1$ due to the relation of pitch-rate-to-pitch as well as pitch-to-altitude by employing differential autopilot for both pitch and altitude loop such that overshoots can be completely eliminated. However, it should be pointed out that exact pole-zero cancellation may not work practically for the reasons given subsequently. This fact also has been proven both experimentally and analytically.
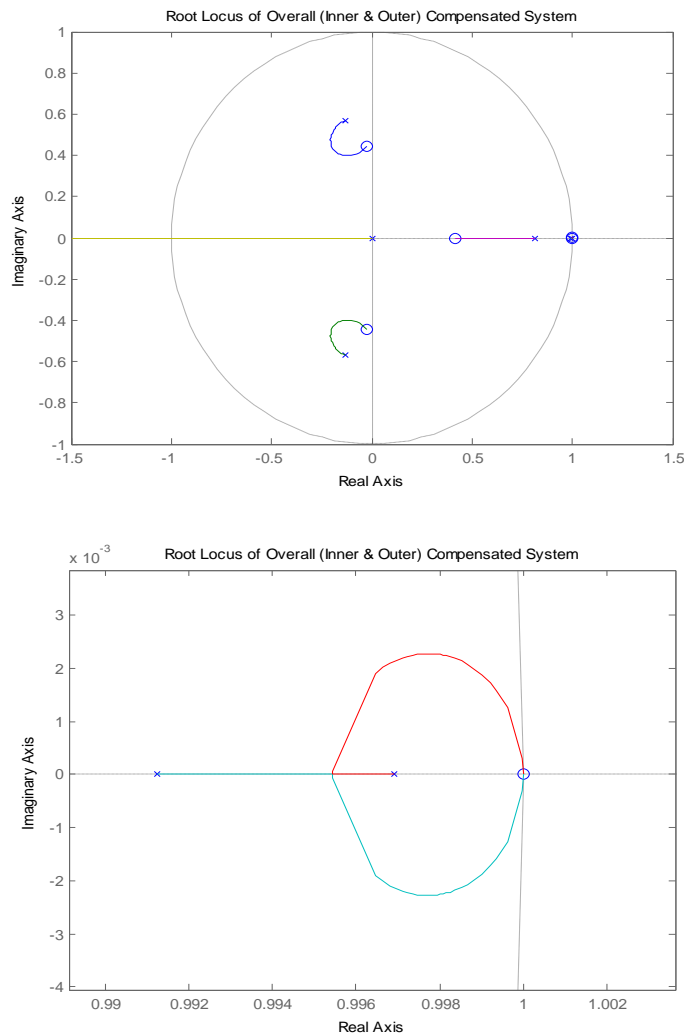
Figure 9 Altitude Root Locus due to D Control.

Firstly, it has been clarified by [9] that exact pole-zero cancellation is impractical due to component tolerances in continuous system and finite word length effect in digital system.

Moreover, the cancelled poles will create the so-called "hidden modes" which may somehow mask the information related to the internal stability [9]. Therefore, even though the controlled variable converges, that is, as

$t \rightarrow \infty$, $y \rightarrow c$, the internal variables within a system may be unbounded, expressed by $t \rightarrow \infty$, $x_i \rightarrow \infty$, should the cancelled poles are unstable.

What is more, from the root locus point of view, it is suspected that the stability issues encountered by employing D controls are due to inescapable path inside the so-called "critical region". It is said to be critical since the root locus branches are located reasonably closed to the stability margin of discrete-time systems $(\Delta < 0.001)$. Hence, regardless the value of the chosen derivative gain, one of the closed loop poles is always trapped there somehow, yields to the unstable closed loop systems as shown by Figure 9.

3.4   Proportional-Integral Autopilot

The mathematical expression of a z domain based PI control is given by:

$$K(z) = K_p + K_i \frac{Tz}{z-1} = \frac{(K_p + K_i T)z - K_p}{(z-1)}, \tag{12}$$

$$= \frac{(K_p + K_i T)\left(z - \dfrac{K_p}{K_p + K_i T}\right)}{z-1}.$$

It turns out that a PI control shall contribute to an additional pole located at

$$z = \frac{K_p}{K_p + K_i T}, \qquad 0 < z < 1,$$

as well as an additional fixed pole at $z = 1$. Thus, One zero needs to be assigned around $z = 1$, therefore, the chosen pitch loop PI control model is depicted in the following equation:

$$K_1(z) = 46.3853\left(\frac{-1.00z + 1}{z - 1}\right). \tag{13}$$

Again, although PI controls shall create zero steady state error, the major drawback of this control scheme is nonetheless related to the existence of overshoots, which is normally higher than PD control.

For pitch PI control loop given by (13), the resulting root locus topology and its unit step responses are given by Figure 10.
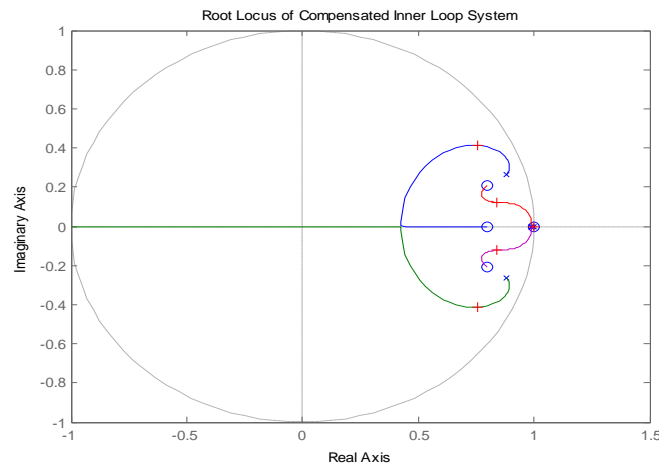
Figure 10 Pitch PI Root Locus.

The inner closed loop poles are given by: $z = 0.7563 \pm 0.4144i$, $z=0.9967$, $z=0.8396 \pm 0.1227i$. It shows a full of 40% overshoot and in fact indicates a more aggressive time domain response, which implies a reasonably higher elevon-average input signal. Moreover, the drawback of the integral control is nonetheless related to the additionally fixed pole at $z = 1$ which tends to destabilise the closed loop control system.
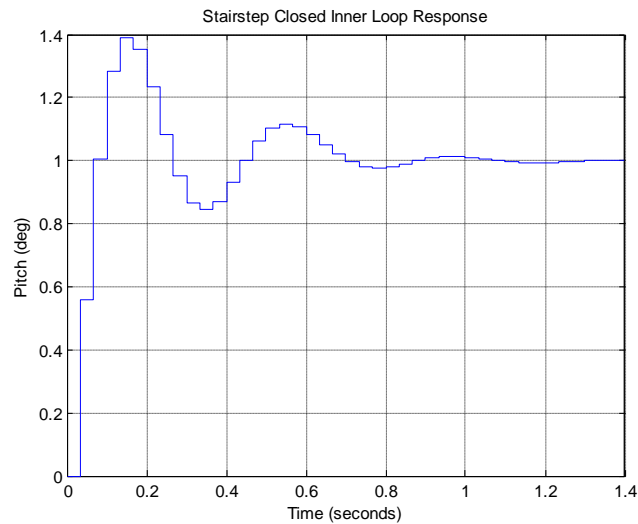

Figure 11 Pitch Response Due to a Unit Step Response.

Similarly, the mathematical model of PI control for the altitude loop is given by:

$$K_2(z) = 5.681\left(\frac{1.04z - 1}{z - 1}\right).\tag{14}$$

The resulting root locus and its closed loop unit step response are given in Figure 12 and Fig 13.
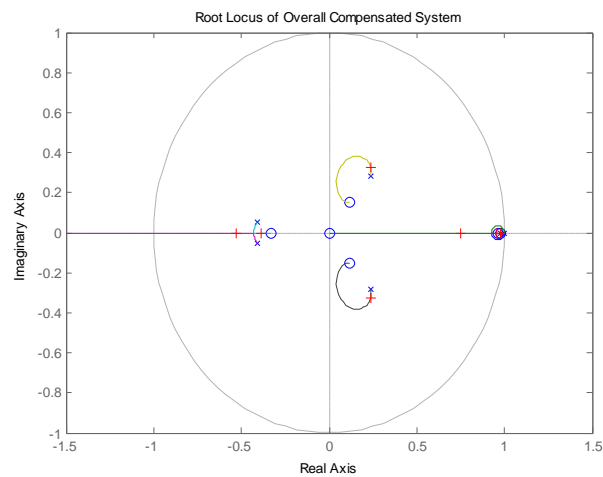

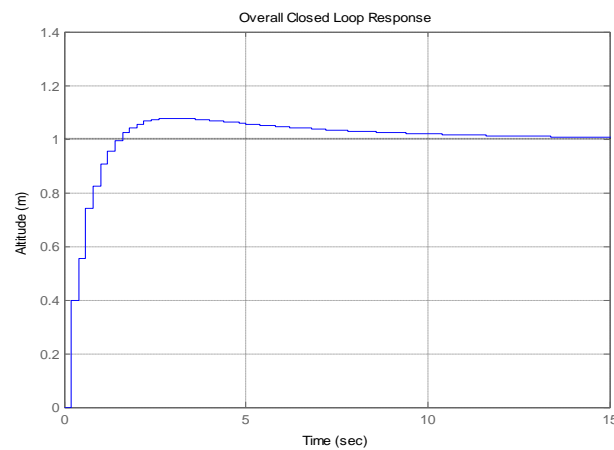**Figure 12**   Altitude Root Locus.

Figure 13   Altitude Step Response.

Furthermore, the resulting altitude loop transfer function is given by:

$$\left.\frac{C(z)}{R(z)}\right|_{5Hz} = \frac{0.39734\, z(z-0.9802)(z-0.9615)(z+0.3272)(z^2-0.2385\, z+0.03743)}{(z+0.5297)(z+0.384)(z-0.7472)(z-0.9559)(z-0.9802)(z^2-0.4758\, x+0.1617)}$$
.
$$(15)$$

In which, its complex conjugate poles are given by: $z=0.2379 \pm 0.3242i$.

The reason why closed loop PI control schemes experience a reasonable amount of overshoots is mainly due to the presence of these complex conjugate poles which are indeed impractical to be completely eliminated. Also, it is obvious from equation (15) that the imaginary parts of the complex conjugate poles are higher than its real parts

3.5   Proportional-Differential Autopilot

In this section, we investigate the performance of PD autopilots in both pitch and altitude control systems. The transfer function of a PD autopilot in z domain can be derived as follows:

$$K(z) = K_p + K_d \frac{(z-1)}{Tz}, \qquad\qquad (16)$$

$$= \frac{K_p T + K_d}{T}\left(\frac{z - \dfrac{K_d}{K_p T + K_d}}{z}\right).$$

By applying this control scheme, one fixed pole at $z = 0$ and one adjustable zero, at $z = \dfrac{K_d}{(K_p T + K_d)}$, are assigned to the open loop system. We can use the additional zero contributed by D control to increase the stability of the closed loop system.

From equation (16), it turns out that the zero satisfies: $0 < \dfrac{K_d}{K_p T + K_d} < 1$, that is, if the total gain is increased, the zero will be shifted to the left. On the other hand, if the total gain is declined, its zero will be shifted to the right. Moreover, it can be predicted that there will be a small amount of steady state error in the system due to the absence of the open loop pole, located at $z = 1$.

The chosen PD control model for pitch loop is given by:

$$K_1(z) = 1.5157\left(\frac{-16z+15}{z}\right). \tag{17}$$

It shall contribute to a new open loop poles at $z = 0$ and a new additional zero at $z = 0.9375$.

Since the altitude transfer function is typically an ideal integrator, due to pitch to altitude factor $z/(z-1)$, consequently, the design objectives of the altitude PD controller is to attract the closed loop poles to move towards inside unit circle as the gain increases. This task can be further accomplished by allocating one zero at $z = 0.333$ as well as one pole at $z = 0$. Accordingly, the mathematical model of the altitude loop autopilot is given by:

$$K_2(z) = 4.7110\left(\frac{1.5z-0.5}{z}\right). \tag{18}$$

Regarding the chosen model of outer loop autopilot, the resulting altitude root locus and its closed loop step response are depicted in Fig 14 and Fig15.

Moreover, the resulting closed loop transfer function is depicted as follow:

$$\left.\frac{C(z)}{R(z)}\right|_{5Hz} = \frac{0.21764(z-0.4751)(z-0.6578)(z-0.3333)(z^2+0.1041z+0.1947)}{(z-0.8287)(z+0.02501)(z^2-1.583z+0.6996)(z^2+0.365z+0.3038)}, \tag{19}$$

In which, its complex conjugate closed loop poles are $z = 0.7913 \pm 0.2709i$ $z = -0.1825 \pm 0.5200i$.
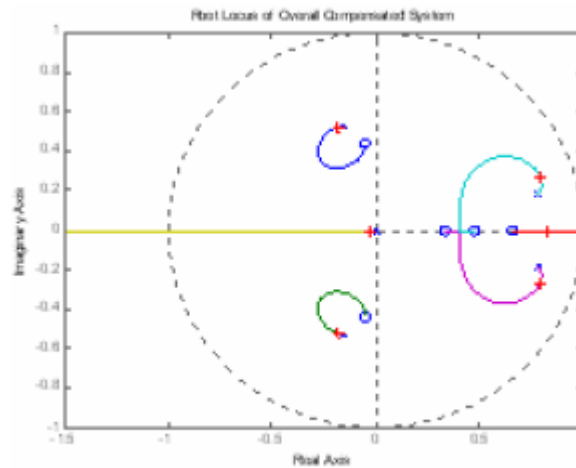

Figure 14 Altitude Root Locus of PD Control.

The altitude root locus of our chosen PD control is given by Figure 14. Subsequently, Figure 15 turns out that the implementation of a PD control yields to a moderately good performances. However, the drawback of this control scheme is nonetheless due to the presence of over/under-shoots and small amount of steady state error.
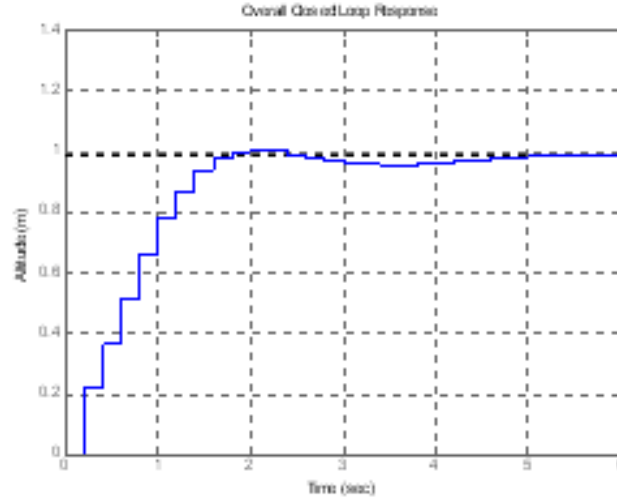

Figure 15   Altitude Unit Step Response due to PD Autopilot Action.

3.6   Complete PID Autopilot Configuration

In this section, the performances of a well-tuned PID control configurations for both pitch and altitude loop are studied. The reason to employ a complete PID control is mainly due to its further flexibility in allocating poles and zeroes offered. This, in general, should lead to the better achievable performance.

The transfer function of a full PID control in z domain can be depicted as follows:

$$K(z) = K_p + K_i \frac{Tz}{z-1} + K_d \frac{z-1}{Tz}, \tag{20}$$

$$= \frac{K_p Tz(z-1) + K_i(Tz)^2 + K_d(z-1)^2}{Tz(z-1)},$$

$$= \frac{(K_p T + K_i T^2 + K_d)z^2 + (-K_p T - 2K_d)z + K_d}{Tz(z-1)}.$$

Thus, it can be regarded as a compensator which shall donate two additionally adjustable zeroes, which depends on its proportional gain K_p, derivative gain K_d, and also integral gain K_i, and two un-adjustable poles located at $z = 0$ and $z = 1$. Mathematically, the allocation of two additional zeroes can be expressed by:

$$z_{1,2} = \frac{(K_p T + 2K_d) \pm \sqrt{(K_p T + 2K_d)^2 - 4(K_p T + K_i T^2 + K_d)K_d}}{2(K_p T + K_i T^2 + K_d)}. \tag{21}$$

Although a full PID control offers more degree of flexibility in allocating poles and zeroes, this will not automatically guarantee a superior performance. To achieve an acceptable performance, its zeros have to be carefully allocated.

In this scenario, the chosen PID autopilot model is given by:

$$K(z) = 47.0785 \left(\frac{-z^2 + 1.6z - 0.6}{z^2 - z} \right). \tag{22}$$

It turns out that:

- The additional zeroes are: $z = 1$ and $z = 0.6$,
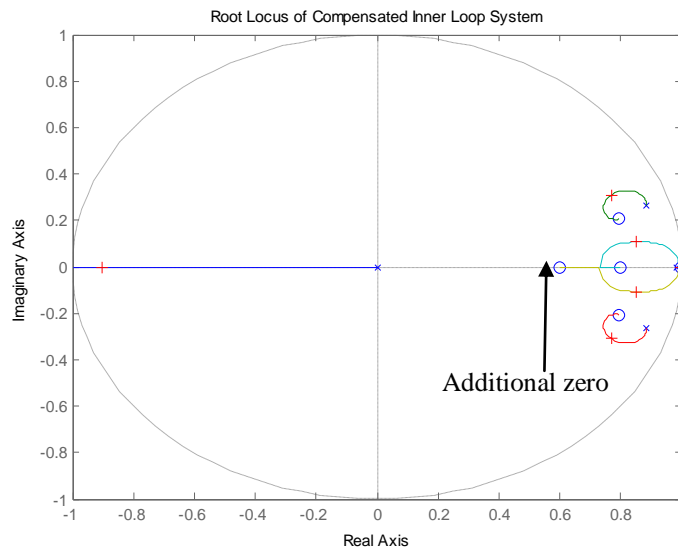- The additional poles are: $z = 1$ and $z = 0$.

Figure 16 Pitch Root Locus for a PID Control.

Therefore, the movements of the root locus branches at $z = 1$ towards the end of its stability margin can be easily hold. Moreover, one new zero at $z = 0.6$ will attract the root locus poles from around $z = 1$, to move closer to left hand side as indicated by the resulting root locus in Fig 16.

Hence the transfer function of the inner closed loop can be depicted as follows:

$$\frac{C_i(z)}{R_i(z)}\bigg|_{30Hz} = \frac{1.4123(z - 0.9967)(z - 0.7989)(z - 0.6012)(z^2 - 1.591z + 0.6755)}{(z + 0.9048)(z - 0.9967)(z^2 - 1.702z + 0.7352)(z^2 - 1.54z + 0.6888)} . \quad (23)$$

In which, its complex conjugate poles are $z = 0.7702 \pm 0.3090i$ as well as $z = 0.8508 \pm 0.1069i$.

Converting into s domain, it becomes:

$$\frac{C_i(s)}{R_i(s)} = \frac{9.9424(s + 540.1)(s + 15.49)(s + 6.694)(s + 0.1003)(s^2 + 11.72s + 91.62)}{(s + 0.1003)(s^2 + 9.226s + 35.35)(s^2 + 11.19s + 162.3)(s^2 + 6s + 8892)}$$

$$(24)$$

Hence, the closed pitch loop transfer function with respect to a 5 Hz sampling is obtained as follows:

$$\frac{C_i(z)}{R_i(z)}\bigg|_{5Hz} = \frac{0.73118(z - 0.9801)(z^2 - 0.7964z + 0.195)(z^2 + 0.2016z + 0.1636)}{(z - 0.9801)(z - 0.5488)(z^2 + 0.4302z + 0.1068)(z^2 - 0.5816z + 0.158)} \quad (25)$$

Equation (25), indicates that there is a pare of common pole and zero that can cancel each other, leading to the following pitch closed loop transfer function:

$$\frac{C_i(z)}{R_i(z)}\bigg|_{5Hz} = \frac{0.73118(z^2 - 0.7964z + 0.195)(z^2 + 0.2016z + 0.1636)}{(z - 0.5488)(z^2 + 0.4302z + 0.1068)(z^2 - 0.5816z + 0.158)} . \quad (26)$$

The pitch closed loop transfer function in equation (25) is obviously the open loop plant for the altitude loop. Its complex conjugate poles are $z = -0.2151 \pm 0.2460i$ as well as $z = 0.2908 \pm 0.2710i$. Furthermore, its complex conjugate zeroes are $z = 0.3982 \pm 0.1909i$ as well as $z = -0.1008 \pm 0.3917i$.

Accordingly, the resulting altitude loop root locus and its unit step response are obtained in Figure17.
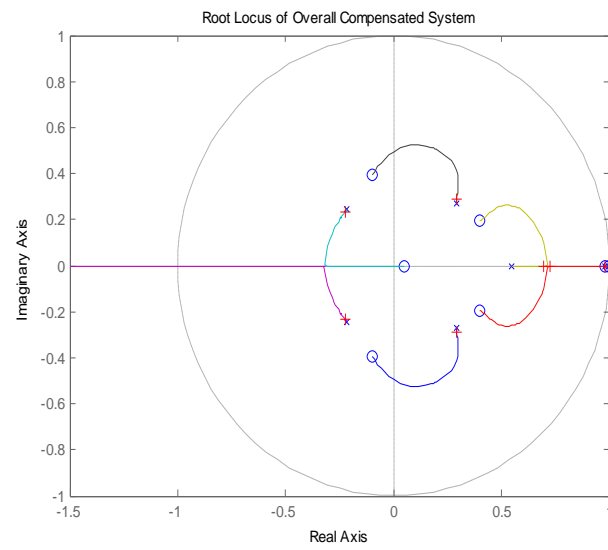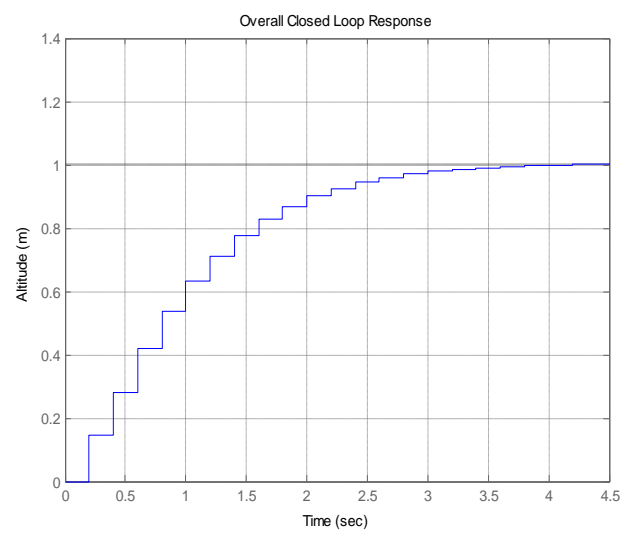
Figure 17   Altitude Root Locus.

Figure 18   Altitude Response.

The overall closed loop transfer function is obtained as follows:

$$\frac{C(z)}{R(z)} = \frac{0.14691(z-0.996)(z-0.9801)(z-0.04763)(z^2-0.7946z+0.195)(z^2+0.2016z+0.1636)}{(z-0.6953)(z-0.7258)(z-0.9801)(z-0.996)(z^2+0.4526z+0.1051)(z^2-0.5858z+0.1705)},$$

in which, its complex conjugate poles are $z = -0.2263 \pm 0.2321i$ as well as $z = 0.929 \pm 0.2911i$.

Thus, a reasonably fast overdamped response (see Figure 18) as indicated by a superior time domain performance has been obtained.

3.6.1   Effects of Disturbances

The purpose of this section is to investigate the performance of the PID autopilots in overcoming the existing disturbances in both pitch and altitude loop. Disturbances were introduced at $t = 20\,s$ and $t = 40\,s$, respectively. Figure 19 obviously indicates that PID autopilots have been able to overcome the disturbances introduced in both pitch and altitude loops at the same time suppress the overshoots in a reasonable time frame.
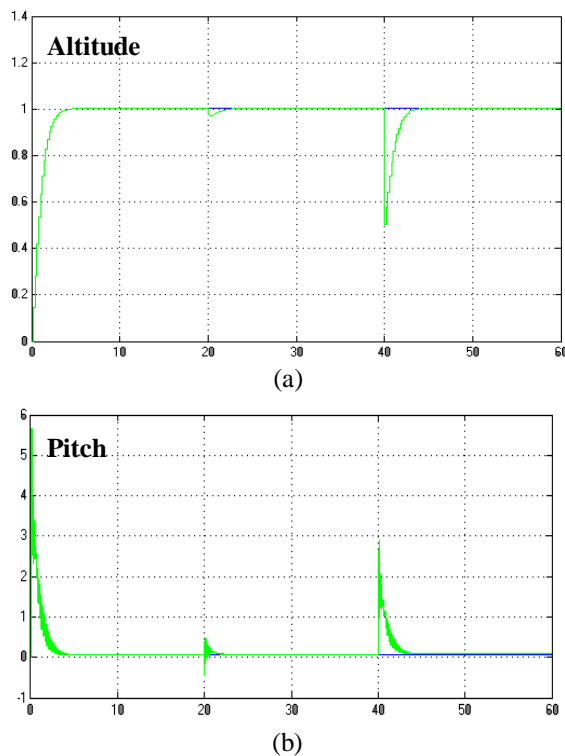

(a)

(b)

Figure 19 Pitch and Altitude Unit Step Responses.

The resulting pitch and altitude loop control signals are depicted in Figure 20.
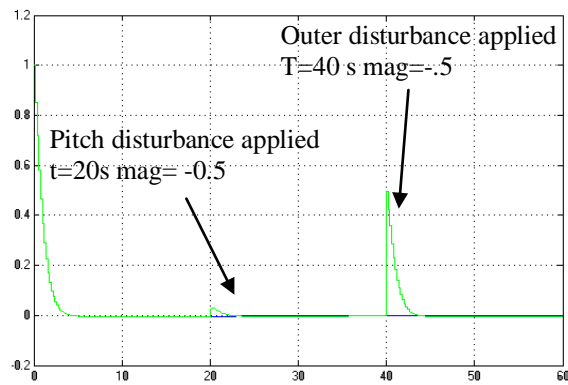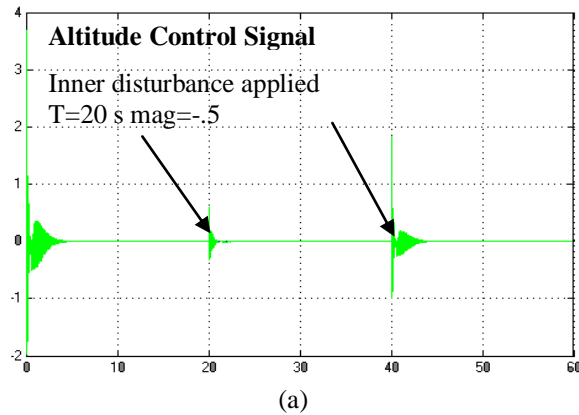
(a)

Figure 20 Pitch and Altitude Control Signals.

It is apparent that as soon as the closed loop system has been successfully stabilised, the control signals were pushed down to zero.

4   Conclusions

A well-tuned PID autopilot has been successfully demonstrated acceptable closed loop performances for both pitch and altitude loops. In general, it can be argued that a full configuration PID autopilot is the suggested control mode to overcome the adverse impacts of disturbances. However, this may lead to a more expensive computational bit for the onboard autopilot.

Overshoots are in fact the undesirable outcomes, particularly, when aircraft wants to land or approach a ground based station. A significant amount of overshoots may lead to the difficulties to land the aircraft or even may cause damage to the whole system. Nevertheless, irrespective of the chosen PID

autopilot gains in both pitch and altitude loops; it is still impractical to completely remove, or achieve an absolutely zero percent overshoots.

The reason for that is because once feedback controls are applied and the gains of the controllers are set to any non zero values, the dominant closed loop poles contributed by OLTF's phugoid modes have been shifted away from the real axis and occupied its imaginary axis. These circumstances are deteriorated by the limitations of the PID control in allocating the desired closed loop poles. Nevertheless, the overshoots still could be minimised into a reasonably safe level

Theoretically, one may argue that D control could be used to cancel double poles at $z = 1$ However; this control scheme only works on papers; for the reasons mentioned in Section 3.3. It also can be further clarified by [9].

Acknowledgement

References

[1]   Santoso F., Liu M. & Egan G.K., H_2 and H_∞ *Robust Autopilot Synthesis for Longitudinal Flight of a Special Unmanned Aerial Vehicle: a Comparative Study*, Institute of Engineering and Technology (IET) Control Theory and Applications, **2**(7), July 2008, pp. 583-594, U.K., [http://www.ietdl.org/].

[2]   Santoso, F., Liu, M. & Egan, G., *Optimal Control Linear Quadratic Synthesis for a UAV*, Proceeding of Twelfth Australian International Aerospace Congress (AIAC-12), Melbourne, 19 -22 March 2007, *also as* MECSE-5-2007, Department of Electrical & Computer Systems Engineering, Monash University, 2006.

[3]   Santoso, F., *Robot Aircraft Dynamics Model Identification and Autopilot Designs*, Master's Thesis, Monash University, 2006.

[4]   Liu, M., Egan, G. & Ge, Y., *Identification of Altitude Flight Dynamics for an Unconventional Aircraft,* Proc. IEEE/RSS International Conference on Intelligent Robotic System (IROS06), Beijing, China, 2006.

[5]   Nasution, S.H, et.al, *GPS-based Altitude and Flight Path Holding System for an Unmanned Aerial Vehicle*. Aerospace Science and Technology Seminar, Jakarta, Indonesia, 21 September 2005.

[6]   Budiyono, A., *Onboard Multivariable Controller Design for a Small Scale Helicopter Using Coefficient Diagram Method*, International Conference on Emerging System Technology, Seoul, Korea 19-20 May 2005.

[7]   Fei-Bin Hsiao et al., *Novel Unmanned Aerial Vehicle System with Autonomous Flight and Auto-Lockup Capability*, 43rd AIAA Aerospace Sciences Meeting and Exhibit 10 - 13 January 2005, Reno, Nevada.

[8]   Turkoglu, K., *Hinf Loop Shaping Robust Control vs. Classical PI(D) Control: A Case Study on the Longitudinal Dynamics of Hezarfen UAV*, Proceedings of the 2nd WSEAS International Conference on Dynamical Systems and Control, Bucharest, Romania, October 16-17, 2006.

[9]   Al-Shamary, N., *Robust and Gain Scheduled Flight Control Systems*, Master of Engineering Science Thesis, Department of Electrical and Computer Systems Engineering, Monash University, 2001.

[10] Kulcsar, B., *LQG/LTR Controller Design for an Aircraft Model*, Periodica   Polytechhica Ser, Vol. 28, No. 1-2, pp 131-142, 2000.

[11] Shahian, B., Hassul, M., *Control System Design Using Matlab ®* , Prentice Hall, Englewood Cliffs, New Jersey, 1993.

[12] Hale, F., *Introduction to Control System Analysis and Design*, Prentice Hall, Englewood Cliffs, NJ, 1988.

[13] Astrom, K., *Automatic Control - the Hidden Technology*, in: Advances in Control: highlights of ECC *'99*, Springer, New York, pp. 1-28, (Chapter 1), 1999.

[14] Forsythe, W., *Digital control: Fundamentals, Theory and Practice*, 1st ed, Macmillan Education, London, 1991.

[15] Franklin, G. F. et al., *Digital Control of Dynamic Systems*,   Addison-Wesley Pub. Co., 1990.

[16] Franklin, G. F, et al., *Feedback Control of Dynamics Systems*, Pearson Prentice Hall, NJ, 2006.

[17] Nise, N., *Control Systems Engineering*, John Willey & Sons, Inc., fourth edition, 2004.

[18] Dutton, K., et al., *The Art of Control Engineering*, Pearson Prenticed Hall, NJ, 1997.

[19] Ogata, K., *Modern Control Engineering*, Prentice Hall, Englewood Cliffs, New Jersey, 1997.

[20] Ogata, K., *Discrete-Time Control Systems*, Prentice Hall, Englewood Cliffs,   New Jersey, 1987.

[21] Ljung, L. and Soderstrom T., *Theory and Practice of Recursive Identification*, MIT Press, 1983.

[22] Ljung, L., System identification toolbox for use with MATLAB, The MathWorks,Inc., 1991.

[23] Ljung, L., *System Identification: Theory for the Users*, Prentice Hall, Englewood Cliffs, New Jersey, 1987.

[24] Juang, J., *Applied system identification*, Prentice Hall, Inc., Englewood Cliffs, New Jersey, 1994.

[25] Goodwin, G. C and Payne, R. L, *Dynamic system identification: Experiment design and data analysis*, Academic Press, INC London, LTD., 1977.

[26] Sage, A. P. and Melsa, J. L., *System Identification*, Academic Press, INC London, LTD., 1971.

[27] Eykhoff, P., System Identification: Parameter and State Estimation, John Wiley & Sons, 1974.

[28] Mehra, R. K. and Lainiotis, D. G., *System Identification Advances and Case Studies*, Academic Press, INC. (London) LTD, 1976.

[29] Bryson, A. J.R., *Control of Spacecraft and Aircraft*, Princeton University Press, NJ, 1994.

[30] Stevens, L B. and Lewis, F., *Aircraft Control and Simulation*, John Wiley & Sons, Inc, 2nd edition, 2003.

[31] Abzug, J. M., Larrabee, E. E., Airplane stability and control: a history of the technologies that made aviation possible.

[32] Etkin, B., *Dynamics of atmospheric flight*, Dover Publications, Inc., 2000.

[33] Cook, M.V., Flight dynamics principles, Arnold, London, 1997.

[34] Pratt. R., *Flight Control Systems: Practical Issues in Design and Implementation*, The Institution of Electrical Engineers, UK, 2000.